



## Article

# Bi-Functional Paraffin@Polyaniline/TiO<sub>2</sub>/PCN-222(Fe) Microcapsules for Solar Thermal Energy Storage and CO<sub>2</sub> Photoreduction

Wenchang Sun, Yueming Hou and Xu Zhang \*

Hebei key Laboratory of Functional Polymers, School of Chemical Engineering and Technology, Hebei University of Technology, Tianjin 300130, China; 201811501015@stu.hebut.edu.cn (W.S.); 201921501013@stu.hebut.edu.cn (Y.H.)

\* Correspondence: xuzhang@hebut.edu.cn; Tel./Fax: +86-22-6020-0443

## 1. Experimental

### 1.1. Chemicals

Aniline (ANI, 98%), methacryloxy propyl trimethoxyl silane (KH-570, 98%), TiO<sub>2</sub> NPs (P25), paraffin (98%, melting point of 50.3 °C), ammonium persulfate (KPS), ZrOCl<sub>2</sub>·8H<sub>2</sub>O (98%), and hydrogen chloride (HCl, 37%) were all purchased from Tianjin Fengchuan Chemical Company. Ethanol (EtOH, 98%), N, N-dimethylformamide (DMF, 98%), and benzoic acid (BA, 98%), Iron(II) chloride tetrahydrate (FeCl<sub>2</sub>·4H<sub>2</sub>O, 99%), anhydrous tetrahydrofuran (THF, 99.5%), propanoic acid (C<sub>2</sub>H<sub>5</sub>COOH, 97%), ethyl acetate (CH<sub>3</sub>COOEt, 98%), potassium hydroxide (KOH, 85%), methyl 4-formylbenzoate (99%), pyrrole (99%), methanol (98%), chloroform (CHCl<sub>3</sub>, 98%) were all purchased from Aladdin Industrial Corporation.

### 1.2. Surface modification of TiO<sub>2</sub> NPs

The surface modification of TiO<sub>2</sub> NPs by KH-570 is described below: 300 mL deionized H<sub>2</sub>O was regulated pH to about four with HCl, then 4 g of TiO<sub>2</sub> was injected in the aqueous solution. The mixture was sonicated for 30 min, then, 3 mL of KH-570 was slowly dripped into the mixture. After that, the mixture was heated up to 80 °C with mechanically stirred for 3 h. Finally, the suspension was collected and washed with H<sub>2</sub>O and EtOH five times, respectively. The modified TiO<sub>2</sub> NPs were obtained after drying at 60 °C overnight.

### 1.3. Ligand Synthesis Procedures.

The ligand was synthesized according to the previous report with some modifications [1,2]. The typical synthetic procedures are described as follows.

#### [5,10,15,20-Tetrakis(4 methoxycarbonylphenyl)porphyrin (TPPCOOMe)]

Typically, pyrrole (3.0 g, 43 mmol), methyl 4 formylbenzoate (6.9 g, 42 mmol), and propionic acid (100 mL) were added to a 500 mL three-necked flask to form a mixed solution, which was then refluxed at 140 °C for 12 h in darkness. After the reaction mixture was cooled down to room temperature, purple crystals were collected by suction filtration. Then the crystals were washed in the sequence of ethanol, ethyl acetate, and THF, and the obtained crystals were dried under vacuum at 60 °C.

#### [5,10,15,20-Tetrakis(4-methoxycarbonylphenyl)porphyrinato]-Fe(III) Chloride (Fe-TPPCOOMe)

Typically, TPP COOMe (0.854 g, 1.0 mmol) was dissolved in DMF solution (100 mL) containing FeCl<sub>2</sub>·4H<sub>2</sub>O (2.5 g, 12.8 mmol) and the mixed solution was refluxed at 160 °C for 6 h. When the mixture was cooled down to room temperature, 150 mL of H<sub>2</sub>O was

added. The resultant precipitate was filtered and washed with 50 mL of H<sub>2</sub>O twice. The obtained solid was dissolved in CHCl<sub>3</sub>, followed by extracting three times with 1 M HCl and twice with water. The organic layer was then dried over anhydrous magnesium sulfate and evaporated to give quantitative dark brown crystals.

#### [5,10,15,20-Tetrakis(4 carboxyphenyl)porphyrinato] Fe(III) Chloride (Fe-TCPP)

The obtained ester (0.75 g) was stirred in THF (25 mL) and MeOH (25 mL) mixed solvent, to which a solution of KOH (2.63 g, 46.95 mmol) in H<sub>2</sub>O (25 mL) was introduced. This mixture was refluxed for 12 h. After cooling down to room temperature, THF and MeOH were evaporated. Additional water was added to the resulting water phase and the mixture was heated until the solid was fully dissolved, then the homogeneous solution was acidified with 1M HCl until no further precipitate was detected. The brown solid was collected by filtration, washed with water, and dried in a vacuum.

#### 1.4. Synthesis of PCN-222(Fe) NPs

The PCN-222(Fe) NPs were synthesized according to the previous report with some modifications [3]. Fe-TCPP (100 mg, 0.13 mmol, the synthesis process see the Supporting Information), 300 mg of ZrOCl<sub>2</sub>·8H<sub>2</sub>O, and 2.2 g of BA were added into 100 mL of DMF, and then the mixture was magnetically stirred (400 rpm) at 90 °C for 4 h. Afterward, PCN-222(Fe) NPs were collected by centrifugation and then washed with DMF three times. The obtained PCN-222(Fe) NPs were dried in a vacuum oven at 120 °C overnight.

#### 1.5. Fabrication of paraffin@PANI/TiO<sub>2</sub>/PCN-222(Fe) (PPTP) MEPCMs

PPTP MEPCMs with TiO<sub>2</sub>/PCN-222(Fe)/PANI ternary hybrid shell were prepared by Pickering emulsion polymerization. The formulas for PPTP MEPCMs are given in **Table S1**. First, the given mass of the TiO<sub>2</sub> and PCN-222(Fe) NPs were put into 120 mL of deionized H<sub>2</sub>O and ultrasonicated for 30 min. Then, paraffin was dispersed in ANI to make up the oil phase. After the mixture of the oil phase and aqueous phase, the mixed liquor was treated with a high-speed disperser at 6000 rpm for 10 min for producing the O/W Pickering emulsion. With a stirring speed of 500 rpm, the emulsion was heated to 75 °C, and then 30 mL H<sub>2</sub>O containing APS was injected dropwise, the reaction was maintained for 4 h. Finally, the products were collected with suction filtration and washed with H<sub>2</sub>O and EtOH two times. The obtained PPTP MEPCMs were dried under vacuum conditions at 60 °C for 8 h.

**Table S1.** Preparation recipes for PPTP MEPCMs.

| Entry | Sample | Paraffin (g) | ANI (mL) | TiO <sub>2</sub> (g) | PCN-222(Fe) (g) | APS (g) |
|-------|--------|--------------|----------|----------------------|-----------------|---------|
| 1     | PPTP-1 | 1.5          | 3        | 0.2                  | 0.1             | 0.4     |
| 2     | PPTP-2 | 1.5          | 1.5      | 0.2                  | 0.1             | 0.2     |
| 3     | PPTP-3 | 1.5          | 0.75     | 0.2                  | 0.1             | 0.1     |
| 4     | PPTP-4 | 1.5          | 0.75     | 0.2                  | 0.05            | 0.1     |
| 5     | PPTP-5 | 1.5          | 0.75     | 0.2                  | 0.025           | 0.1     |

## 2. Characterization

Fourier transform infrared spectrometer (Bruker VECTOR-22) was used for collecting FT-IR spectra with KBr pellet method. The X-ray diffraction (XRD) patterns of the materials were collected by X-ray powder diffractometer (Bruker D8 Davinci) with Cu K $\alpha$  radiation (40 kV, 150 mA) at the rate of 5° min<sup>-1</sup>. X-ray photoelectron spectroscopy spectra were obtained by X-ray photoelectric spectrometer (XPS, Thermo Scientific ESCA-Lab250Xi), and the spot size was 650  $\mu$ m. The binding energy was calibrated using a C 1s peak of 284.6 eV. Scanning electron microscope characterization was performed using field emission scanning electron microscopy (SEM, FEI Nova Nano-SEM450) with an acceleration voltage of 1 kV, and the surface elemental compositions were carried out by an energy-dispersive X-ray (EDX) spectrometer coupled with an acceleration voltage of 10

kV. Transmission electron microscopy (TEM) was acquired on the FEI Talos F200S. The  $N_2$  adsorption-desorption curve and pore structure characteristics were obtained by specific surface area and porosity analyzer (ASAP 2020 M+C), and the pore size was calculated by the Brunauer-Emmett-Teller (BET) method. The thermal analysis was carried out by a differential scanning calorimeter (DSC, TA Discovery) at temperatures ranging from 0 to 80 °C with a heating/cooling rate of  $\pm 5$  °C/min<sup>-1</sup> and under an  $N_2$  atmosphere at a flow rate of 60 mL·min<sup>-1</sup>. 500 melting-cooling cycle tests were carried out in a high and low-temperature test chamber (THS-250B, China) to evaluate the leakage property and cyclability. The heating range was 10 ~ 60 °C with a rate of 4 °C·min<sup>-1</sup>, the cooling range was 60 ~ 10 °C with a rate of -1 °C·min<sup>-1</sup>. The thermal stability of the samples was measured by thermal gravimetric analysis (TGA, SDT/Q600) under airflow with a heating rate of 10 °C·min<sup>-1</sup> from 20 to 800 °C. The UV-Vis diffuse reflectance spectra (DRS) of the materials were obtained using the UV-Vis spectrophotometer (HITACHI, U-3900H) and  $BaSO_4$  as the substrate. The sunlight was simulated by a 300 W xenon lamp (Irradiate the test materials at  $\lambda > 300$  nm) to perform the photothermal conversion measurement. The materials were placed on the plate (10 × 10 cm<sup>2</sup>), a thermocouple and TETO IR software were used to record the temperature change of the samples. At the same time, the xenon lamp was used to irradiate the materials, and an infrared thermal imager (ST9550) was employed to record the surface temperature every 30 s.

### 3. Electrochemical test

The electrochemical properties of the materials were tested by Tianjin Lanlike electrochemical workstation (LK2010). The standard three-electrode method was adopted in the test process, in which Ag/AgCl (saturated KCl) was used as the reference electrode and platinum foil (Pt) electrode was used as the counter electrode. In the test of electrochemical impedance spectroscopy (EIS), the catalyst samples suspension droplets were coated on carbon paper as working electrodes, and the electrolyte was  $Na_2SO_4$  solution (0.5 M). In the photocurrent test, the catalyst samples suspension droplets were coated on FTO glass as working electrodes, and the electrolyte was  $Na_2SO_4$  solution (0.5 M). Then, the electrodes were dried in an oven. During the electrochemical test, the same light source as in the reaction was used for the test. Under the bias voltage of -0.5 V, the photocurrent curves were obtained by opening/masking the light source every 20 s. The electrochemical impedance spectroscopy (EIS) curves were measured at a frequency range of  $10^{-1} \sim 10^{-5}$  Hz, and an alternating voltage of 10 mV. Mott-Schottky curves were measured in the dark at 1000 Hz.

### 4. Photocatalytic reaction of $CO_2$

A 300 W xenon lamp ( $\lambda > 300$  nm, Beijing, China, Perfect light Technology Co., Ltd.) was employed as the irradiation light source, and fixed 10 cm away from the sample. Firstly, 6 mL of deionized  $H_2O$  and 0.2 g of catalyst were injected into the quartz glass reactor, high-purity  $CO_2$  (0.1 MPa) was filled, and vacuum treatment was carried out twice to completely remove impurities. During the reaction, the gas product was determined by a gas chromatograph (GC-7920, Beijing, China, Zhongjiao Jinyuan Technology Co., Ltd.) with flame ionization detector FID and Ar as the carrier gas. For the subsequent recycling test, the photocatalyst after the reaction was recovered by filtration, washed three times with  $H_2O$  and ethanol, and then dried in a vacuum oven for 10 h at 60 °C. The recycle test of PPTP-3 was consistent with the above test conditions, and the recycle test times were set as 5 times.

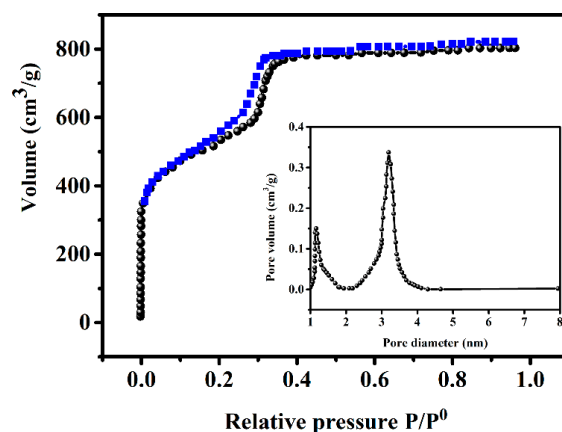


**Figure S1.** N<sub>2</sub> adsorption-desorption isotherms and the corresponding pore-size distributions (inset) of PCN-222(Fe) NPs.

Calculation formula of  $E_{en}$ ,  $E_{es}$ , and  $C_{es}$ :

$$E_{en} = \frac{\Delta H_{m, MEPCMs}}{\Delta H_{m, paraffin}} \times 100\% \quad \text{Equation (S1)}$$

$$E_{es} = \frac{\Delta H_{m, MEPCMs} + \Delta H_{c, MEPCMs}}{\Delta H_{m, paraffin} + \Delta H_{c, paraffin}} \times 100\% \quad \text{Equation (S2)}$$

$$C_{es} = \frac{\Delta H_{m, MEPCMs} + \Delta H_{c, MEPCMs}}{(\Delta H_{m, paraffin} + \Delta H_{c, paraffin}) \times E_{en}} \times 100\% \quad \text{Equation (S3)}$$

Where  $\Delta H_m$ , melting enthalpy;  $\Delta H_c$ , crystallization enthalpy;  $E_{en}$ , encapsulation efficiency;  $E_{es}$ , energy storage efficiency; and  $C_{es}$ , thermal storage capability.

**Table S2.** Performance comparison of microencapsulated PCMs with organic-inorganic hybrid shell in the literature.

| Sample   | Preparation Methods  | Co-emulsifier   | $\Delta H_m^a$<br>(J·g <sup>-1</sup> ) | $E_{en}^b$<br>(%) | Thermal<br>cycles<br>times | Loss of<br>$\Delta H_m$<br>(J·g <sup>-1</sup> ) | Additional function                | Refer-<br>ences |
|--|--|-----------------|--|-------------------|----------------------------|---|------------------------------------|-----------------|
| PCM@MgO/TiO <sub>2</sub> /Graphite/PS                | Emulsion polymerization  | SDS             | N                                      | 69.9              | N                          | N   | N                                  | [4]             |
| PCM@MF/SiO <sub>2</sub>                              | Emulsion polymerization  | No              | 167.1                                  | N                 | 100                        | Slightly  | N                                  | [5]             |
| PCM@poly(4-MeS-co-DVB)/TiO <sub>2</sub>              | Suspension polymerization  | No              | 174                                    | 76.6              | 100                        | Slightly  | Photodegradation of methylene blue | [6]             |
| PCM@SiO <sub>2</sub> /TiO <sub>2</sub> /PDA          | In-situ polymerization   | CTAB            | 125.9                                  | N                 | N                          | N   | Solar-thermal energy conversion    | [7]             |
| PCM@thermochromic pigment/PMMA                       | Suspension-like polymerization                                     | TA              | 129.7                                  | 66.3              | N                          | N   | Thermochromic property             | 8               |
| PCM@poly(HDDA)/TiO <sub>2</sub>                      | On-the-fly photopolymerization                                     | No              | N                                      | N                 | N                          | N   | MB Photodegradation                | 9               |
| PCM@Fe <sub>3</sub> O <sub>4</sub> /SiO <sub>2</sub> | Pickering emulsion polymerization and interfacial polycondensation | CTAB            | 169.6                                  | 71.8              | 100                        | Slightly  | Magnetism                          | 10              |
| PCM@PMMA/PMA/Si <sub>3</sub> N <sub>4</sub>          | Pickering emulsion polymerization                                  | SDBS            | 134.6                                  | 79.9              | N                          | N   | No                                 | 11              |
| PCM@PDA/SiO <sub>2</sub> /Ag                         | Interfacial co-hydrolysis and condensation & electroless plating   | CTAB            | 106.5                                  | N                 | 100                        | Severely  | No                                 | 12              |
| PCM@graphene/MF                                      | In-situ polymerization   | PVA and PEG-800 | 219.9                                  | 86.54             | N                          | N   | No                                 | 13              |
| PCM@PU/TiO <sub>2</sub>                              | Interfacial polymerization   | PEG             | 147.7                                  | 83.3              | 30                         | Slightly  | No                                 | 14              |
| PCM/PMMA/PBA/TiO <sub>2</sub>                        | Pickering emulsion polymerization                                  | No              | 90.1                                   | 36.0              | N                          | N   | No                                 | 15              |
| PCM@PMMA/TiC/SiO <sub>2</sub>                        | Pickering emulsion polymerization                                  | No              | 93.0                                   | N                 | N                          | N   | No                                 | 16              |
| PCM@PDVB/SiO <sub>2</sub>                            | Sol-gel and graft polymerization                                   | CTAB            | 199.6                                  | 80.0              | N                          | N   | No                                 | 17              |
| PCN-222(Fe)/PANI/TiO <sub>2</sub>                    | Pickering emulsion polymerization                                  | No              | 174.7                                  | 77.2              | 500                        | Slightly  | CO <sub>2</sub> Photoreduction     | This work       |

Note: <sup>a</sup> the melting enthalpy, <sup>b</sup> the encapsulation efficiency, N- Not mentioned.

**Table S3.** Performance comparison of ternary heterojunction photocatalysts in the literature.

| Ternary heterojunction  | Reductant                          | Light source                           | Generation rate of main products ( $\mu\text{mol}\cdot\text{g}^{-1}\cdot\text{h}^{-1}$ ) | References |
|---|------------------------------------|--|--|------------|
| CdS/rGO/TiO <sub>2</sub>  | H <sub>2</sub> O vapor             | 300 W<br>Xe lamp                       | CH <sub>4</sub> : 0.12   | 18         |
| CuGaS <sub>2</sub> -RGO-TiO <sub>2</sub>                              | Na <sub>2</sub> S aqueous solution | 300 W<br>Xe lamp ( $\lambda > 330$ nm) | CO: 0.15   | 19         |
| g-C <sub>3</sub> N <sub>4</sub> /Pt/3DOM-TiO <sub>2</sub> @C          | H <sub>2</sub> O vapor             | 300 W Xe lamp ( $\lambda \geq 420$ nm) | CO: 1.47<br>CH <sub>4</sub> : 6.56   | 20         |
| (Au/A-TiO <sub>2</sub> )@g-C <sub>3</sub> N <sub>4</sub>              | H <sub>2</sub> O vapor             | 300 W Xe lamp ( $\lambda \geq 420$ nm) | CO: 21.7<br>CH <sub>4</sub> : 37.4   | 21         |
| WO <sub>3</sub> -TiO <sub>2</sub> /Cu <sub>2</sub> ZnSnS <sub>4</sub> | H <sub>2</sub> O vapor             | 400 W Xe lamp ( $\lambda > 420$ nm)    | CO: 15.37<br>CH <sub>4</sub> : 1.69  | 22         |
| PtRu/TiO <sub>2</sub>   | H <sub>2</sub> O vapor             | 300 W<br>Xe lamp                       | CO: 2.6<br>CH <sub>4</sub> : 38.7  | 23         |
| CNT/TiO <sub>2</sub> /Cu  | H <sub>2</sub> O vapor             | 300 W<br>Xe lamp                       | CO: 8.1<br>CH <sub>4</sub> : 1.1   | 24         |
| Au/Al <sub>2</sub> O <sub>3</sub> /TiO <sub>2</sub>                   | H <sub>2</sub> O vapor             | 450 W Xe lamp                          | CO: 11.8   | 25         |
| PCN-222(Fe)/PANI/TiO <sub>2</sub>                                     | H <sub>2</sub> O vapor             | 300 W<br>Xe lamp ( $\lambda > 300$ nm) | CO: 45.16<br>CH <sub>4</sub> : 0.39  | This work  |

## References

- Feng, D.; Gu, Z.-Y.; Li, J.-R.; Jiang, H.-L.; Wei, Z.; Zhou, H. Zirconium-metalloporphyrin PCN-222: mesoporous metal-organic frameworks with ultrahigh stability as biomimetic catalysts. *Angew. Chem. Int. Ed.* **2012**, *51*, 10307–10310, <https://doi.org/10.1002/anie.201204475>.
- Asano, N.; Uemura, S.; Kinugawa, T.; Akasaka, H.; Mizutani, T. Synthesis of biladienone and bilatrienone by coupled oxidation of tetraarylporphyrins. *J. Org. Chem.* **2007**, *72*, 5320–5326, <https://doi.org/10.1021/jo070692a>.
- Park, J.; Jiang, Q.; Feng, D.; Mao, L.; Zhou, H.-C. Size-controlled synthesis of porphyrinic metal-organic framework and functionalization for targeted photodynamic therapy. *J. Am. Chem. Soc.* **2016**, *138*, 3518–3525, <https://doi.org/10.1021/jacs.6b00007>.
- Sami, S.; Etesami, N. Heat transfer enhancement of microencapsulated phase change material by addition of nanoparticles for a latent heat thermal energy storage system. *Energy Rep.* **2021**, *7*, 4930–4940, <https://doi.org/10.1016/j.egy.2021.07.080>.
- Zhai, D.; He, Y.; Zhang, X.; Li, W. Preparation, Morphology, and thermal performance of microencapsulated phase change materials with a MF/SiO<sub>2</sub> composite shell. *Energy Fuels* **2020**, *34*, 16819–16830, <https://doi.org/10.1021/acs.energyfuels.0c03121>.
- Parvate, S.; Singh, J.; Dixit, P.; Vennapusa, J.R.; Maiti, T.K.; Chattopadhyay, S. Titanium Dioxide Nanoparticle-Decorated Polymer Microcapsules Enclosing Phase Change Material for Thermal Energy Storage and Photocatalysis. *ACS Appl. Polym. Mater.* **2021**, *3*, 1866–1879, <https://doi.org/10.1021/acsapm.0c01410>.
- Pornea, A.M.; Kim, H. Design and synthesis of SiO<sub>2</sub>/TiO<sub>2</sub>/PDA functionalized phase change microcapsules for efficient solar-driven energy storage. *Energy Convers. Manag.* **2021**, *232*, 113801.
- Wang, H.; Luo, J.; Yang, Y.; Zhao, L.; Song, G.; Tang, G. Fabrication and characterization of microencapsulated phase change materials with an additional function of thermochromic performance. *Sol. Energy* **2016**, *139*, 591–598, <https://doi.org/10.1016/j.solener.2016.10.011>.
- Ruqaiya, A.N.; Guido, B.; Vladislavljjevic, G.T. Microfluidic production of poly(1,6-hexanediol diacrylate)-based polymer microspheres and bifunctional microcapsules with embedded TiO<sub>2</sub> nanoparticles. *Langmuir* **2018**, *34*, 11822–11831, <https://doi.org/10.1021/acs.langmuir.8b02452>.
- Jiang, F.; Wang, X.; Wu, D. Design and synthesis of magnetic microcapsules based on *n*-eicosane core and Fe<sub>3</sub>O<sub>4</sub>/SiO<sub>2</sub> hybrid shell for dual-functional phase change materials. *Appl. Energy* **2014**, *134*, 456–468, <https://doi.org/10.1016/j.apenergy.2014.08.061>.
- Sun, N.; Xiao, Z. Paraffin wax-based phase change microencapsulation embedded with silicon nitride nanoparticles for thermal energy storage. *J. Mater. Sci.* **2016**, *51*, 8550–8561, <https://doi.org/10.1007/s10853-016-0116-0>.
- Zhu, Y.; Chi, Y.; Liang, S.; Luo, X.; Chen, K.; Tian, C.; Wang, J.; Zhang, L. Novel metal coated nanoencapsulated phase change materials with high thermal conductivity for thermal energy storage. *Sol. Energy Mater. Sol. Cells* **2017**, *176*, 212–221, <https://doi.org/10.1016/j.solmat.2017.12.006>.
- Zhao, Q.; He, F.; Zhang, Q.; Fan, J.; He, R.; Zhang, K.; Yan, H.; Yang, W. Microencapsulated phase change materials based on graphene Pickering emulsion for light-to-thermal energy conversion and management. *Sol. Energy Mater. Sol. Cells* **2019**, *203*, 110204, <https://doi.org/10.1016/j.solmat.2019.110204>.
- Wang, Z.; Ma, W.; Hu, D.; Wu, L. Synthesis and characterization of microencapsulated methyl laurate with polyurethane shell materials via interfacial polymerization in Pickering emulsions. *Colloids Surfaces A: Physicochem. Eng. Asp.* **2020**, *600*, 124958, <https://doi.org/10.1016/j.colsurfa.2020.124958>.
- Qiu, X.Z.; Tao, Y.; Xu, X.Q.; He, X.H.; Fu, X.Y. Synthesis and characterization of paraffin/TiO<sub>2</sub>-P(MMA-co-BA) phase change material microcapsules for thermal energy storage. *J. Appl. Polym. Sci.* **2018**, *135*, <https://doi.org/10.1002/app.46447>.
- Wang, H.; Zhao, L.; Song, G.; Tang, G.; Shi, X. Organic-inorganic hybrid shell microencapsulated phase change materials prepared from SiO<sub>2</sub>/TiC-stabilized Pickering emulsion polymerization. *Sol. Energy Mater. Sol. Cells* **2018**, *175*, 102–110, <https://doi.org/10.1016/j.solmat.2017.09.015>.

17. Ji, X.; Chen, J.; Dang, G.; Zhang, Y.; Yang, J.; Li, W.; Zhao, Y.; Jin, Z. Preparation of phase change microcapsules with inorganic/polymer hybrid shell through a “two-step” reaction. *Polym. Sci. Ser. B* **2019**, *61*, 560–566, <https://doi.org/10.1134/s1560090419050075>.
18. Kuai, L.; Zhou, Y.; Tu, W.; Li, P.; Li, H.; Xu, Q.; Tang, L.; Wang, X.; Xiao, M.; Zou, Z. Rational construction of a CdS/reduced graphene oxide/TiO<sub>2</sub> core–shell nanostructure as an all-solid-state Z-scheme system for CO<sub>2</sub> photoreduction into solar fuels. *RSC Adv.* **2015**, *5*, 88409–88413, <https://doi.org/10.1039/c5ra14374h>.
19. Takayama, T.; Sato, K.; Fujimura, T.; Kojima, Y.; Iwase, A.; Kudo, A. Photocatalytic CO<sub>2</sub> reduction using water as an electron donor by a powdered Z-scheme system consisting of metal sulfide and an RGO-TiO<sub>2</sub> composite. *Faraday Discuss.* **2017**, *198*, 397–407, <https://doi.org/10.1039/C6FD00215C>.
20. Wang, C.; Liu, X.; He, W.; Zhao, Y.; Wei, Y.; Xiong, J.; Liu, J.; Li, J.; Song, W.; Zhang, X.; et al. All-solid-state Z-scheme photocatalysts of g-C<sub>3</sub>N<sub>4</sub>/Pt/macroporous-(TiO<sub>2</sub>@carbon) for selective boosting visible-light-driven conversion of CO<sub>2</sub> to CH<sub>4</sub>. *J. Catal.* **2020**, *389*, 440–449, <https://doi.org/10.1016/j.jcat.2020.06.026>.
21. Wang, C.; Zhao, Y.; Xu, H.; Li, Y.; Wei, Y.; Liu, J.; Zhao, Z. Efficient Z-scheme photocatalysts of ultrathin g-C<sub>3</sub>N<sub>4</sub>-wrapped Au/TiO<sub>2</sub>-nanocrystals for enhanced visible-light-driven conversion of CO<sub>2</sub> with H<sub>2</sub>O. *Appl. Catal. B: Environ.* **2019**, *263*, 118314, <https://doi.org/10.1016/j.apcatb.2019.118314>.
22. Raza, A.; Shen, H.; Haidry, A.A.; Sun, L.; Liu, R.; Cui, S. Studies of Z-scheme WO<sub>3</sub>-TiO<sub>2</sub>/Cu<sub>2</sub>ZnSnS<sub>4</sub> ternary nanocomposite with enhanced CO<sub>2</sub> photoreduction under visible light irradiation. *J. CO<sub>2</sub> Util.* **2020**, *37*, 260–271, <https://doi.org/10.1016/j.jcou.2019.12.020>.
23. Wei, Y.; Wu, X.; Zhao, Y.; Wang, L.; Zhao, Z.; Huang, X.; Liu, J.; Li, J. Efficient photocatalysts of TiO<sub>2</sub> nanocrystals-supported PtRu alloy nanoparticles for CO<sub>2</sub> reduction with H<sub>2</sub>O: Synergistic effect of Pt-Ru. *Appl. Catal. B: Environ.* **2018**, *236*, 445–457, <https://doi.org/10.1016/j.apcatb.2018.05.043>.
24. Rodríguez, V.; Camarillo, R.; Martínez, F.; Jiménez, C.; Rincón, J. CO<sub>2</sub> photocatalytic reduction with CNT/TiO<sub>2</sub> based nanocomposites prepared by high-pressure technology. *J. Supercrit. Fluids* **2020**, *163*, 104876, <https://doi.org/10.1016/j.supflu.2020.104876>.
25. Zhao, H.; Zheng, X.; Feng, X.; Li, Y. CO<sub>2</sub> Reduction by plasmonic Au nanoparticle-decorated TiO<sub>2</sub> photocatalyst with an ultrathin Al<sub>2</sub>O<sub>3</sub> interlayer. *J. Phys. Chem. C* **2018**, *122*, 18949–18956, <https://doi.org/10.1021/acs.jpcc.8b04239>.